DYNA
http://dyna.medellin.unal.edu.co/

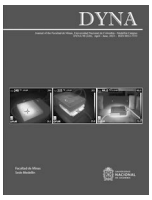

UNIVERSIDAD NACIONAL DE COLOMBIA

Low organic content hybrid perovskite $(Cs_{1-x}DMA_x)Pb(Br_{1-x}I_x)_3$ with increased stability for solar cell fabrication

Juan José Patiño-López, Juan Felipe Montoya-Arango, Edwin Alexander Ramírez-Pérez, Franklin Jaramillo-Isaza & Daniel Estiben Ramirez-Zora

Centro de Investigación, Innovación y Desarrollo de Materiales – CIDEMAT, Facultad de Ingeniería, Universidad de Antioquia, Medellín, Colombia.
juan.patino11@udea.edu.co, felipe.montoya@udea.edu.co, ramirezp.edwin@gmail.com, franklin.jaramillo@udea.edu.co, estiben.ramirez@udea.edu.co

Received: November 29th, 2022. Received in revised form: April 19th, 2023. Accepted: May 8th, 2023

Abstract
Hybrid perovskites with reduced organic content have brought great interest for solar cells applications. Particularly, adding inorganic cations increase material stability, by providing an adequate tolerance factor. However, these cations lead to lower absorption coefficient than using only organic cations, therefore it is necessary to implement strategies for having films with appropriate thickness and good light absorption properties. In this work, several experiments were performed with $((Cs_{1-x}DMA_x)Pb(Br_{1-x}I_x)_3$ perovskite films of different thicknesses, resulting in devices with photovoltaic conversion efficiency (PCE) near 80% of the reference $MAPbI_3$ cell, high purity phase, appropriate morphology, and higher stability. The perovskite successfully maintained integrity for 12 days in air with relative humidity between 30 and 40%, indicating the fulfillment of the study's objectives.

Key words: solar cells; renewable energy; hybrid perovskite; inorganic cations; tolerance factor; stability.

Perovskita híbrida de bajo contenido orgánico $(Cs_{1-x}DMA_x)Pb(Br_{1-x}I_x)_3$ con estabilidad aumentada para la fabricación de celdas solares

Resumen
Las perovskitas híbridas con contenido orgánico reducido han despertado gran interés en aplicaciones de celdas solares. En particular, la adición de cationes inorgánicos aumenta la estabilidad del material al proporcionar un factor de tolerancia adecuado. Sin embargo, estos cationes llevan a un coeficiente de absorción menor que al usar solo solo cationes orgánicos, por lo tanto, es necesario implementar estrategias para obtener películas con un espesor adecuado y buenas propiedades de absorción de luz. En este trabajo se realizaron varios experimentos con películas de perovskita $((Cs_{1-x}DMA_x)Pb(Br_{1-x}I_x)_3)$ de diferentes espesores, lo que resultó en dispositivos con una eficiencia de conversión fotovoltaica (PCE) cercana al 80% de la celda de referencia $MAPbI_3$, fase de alta pureza, morfología adecuada y mayor estabilidad. La perovskita mantuvo su integridad con éxito durante 12 días en aire con una humedad relativa entre el 30 y el 40%, lo que indica el cumplimiento de los objetivos del estudio.

Palabras clave: celdas solares; energía renovable; perovskita híbrida; cationes inorgánicos; factor de tolerancia; estabilidad.

1 Introduction

One of the most important challenges facing humanity today is the reduction of pollution generated using fossil fuels. To meet this challenge, solar photovoltaic (PV) is a clean energy generation alternative, with very low levels of greenhouse gas emissions in operation and significant reduction of the levelized cost of electricity (LCOE). Between 2010 and 2020, the LCOE of PV plants was reduced by 85%, from 0.381 USD/kilowatt hour (kWh) to 0.057 USD/kWh in 2020 [1].

Historically, silicon has been the most widely used

How to cite: Patiño-López, J.J., Montoya-Arango, J.F., Ramírez-Pérez, E.A., Jaramillo-Isaza, F. and Ramirez-Zora, D.E., Low organic content hybrid perovskite (Cs1-xDMAx)Pb(Br1-xIx)3 with increased stability for solar cell fabrication. DYNA, 90(226), pp. 83-89, April - June, 2023.

© The author; licensee Universidad Nacional de Colombia.

semiconductor in the photovoltaic industry due to abundantly available raw materials, stability and no apparent environmental health or safety issues. However, perovskite has several advantages over Si cells, as they are compatible with scalable printing fabrication methods and have a high absorption coefficient that facilitates the production of thin, light and even flexible devices [2]. These advantages make perovskite technology promising for niche markets such as: building integrated photovoltaics (BIPV), agrovoltaics, flexible devices, IoT, among others [2]. Recently, perovskite solar cells with an energy conversion efficiency (PCE) of 25.8% have been fabricated at laboratory scale, which is close to the maximum efficiency achieved with Si cells. But these highly efficient devices can only maintain 90% of their initial efficiency for 500 hours of illumination, which calls for research into strategies to increase temporal stability under real-world operating conditions.

Recent reports have shown that the decrease or replacement of organic cations (e.g., $CH_3NH_3^+$ in $MAPbI_3$ which is the most studied perovskite because of its simple composition and processability) by an inorganic cation such as Cs^+ improves thermal stability [3]. Z. Li *et al.,* developed a structure with 10% Cs^+ ions ($FA_{0.9}Cs_{0.1}PbI_3$), achieving an efficiency of 23.21% which maintains 80% of its initial efficiency after 500 h of continuous light soaking [4]. X. Zhu *et al*., incorporated 23% of Cs in the $MA_{1-x}Cs_xPbI_3$ structure, achieving a cell efficiency of 20.13% and the devices stored in the dark for one year decreased only 4.37% of the initial efficiency [5]. G. Tong *et al*., fabricated a totally inorganic perovskite with the Br^{-1} anion ($CsPbBr_3$) and achieved a PCE of 10.91% which maintains 90% of initial PCE after 1000 h and 80% of initial PCE after 2000 h in conditions of 45% relative humidity and 100 °C [6]. Yixin Zhao et al., achieved a PCE of 19.03% in a device with the perovskite structure $CsPbI_3$ which exhibited good photo-stability and retained 90% of their initial PCE after 500 h of continuous illumination [7]. Chunfu Zhang et al., fabricated a full inorganic perovskite with the structure $CsPbI_2Br$, achieving a PCE of 19.3% which maintains 41.9% of its initial PCE even in deep water [8]. This research demonstrates the possibility of having perovskite solar cells with remarkable improvements in stability due to the incorporation of inorganic cations.

There are several ways to increase the stability of perovskites under different environmental conditions. One of them is to promote structural stability between the cations and anions that make up the ABX_3 crystal. Goldschmidt tolerance factor (t) is a ratio that helps to calculate the preferential structure formed depending on the cations and anions used as shown in eq. (1) where R is the radius of each component in the structure. By tuning the t-factor it is possible to find the conditions for the structure to remain in the desired alpha-cubic phase for a long time (Fig. 1) [9].

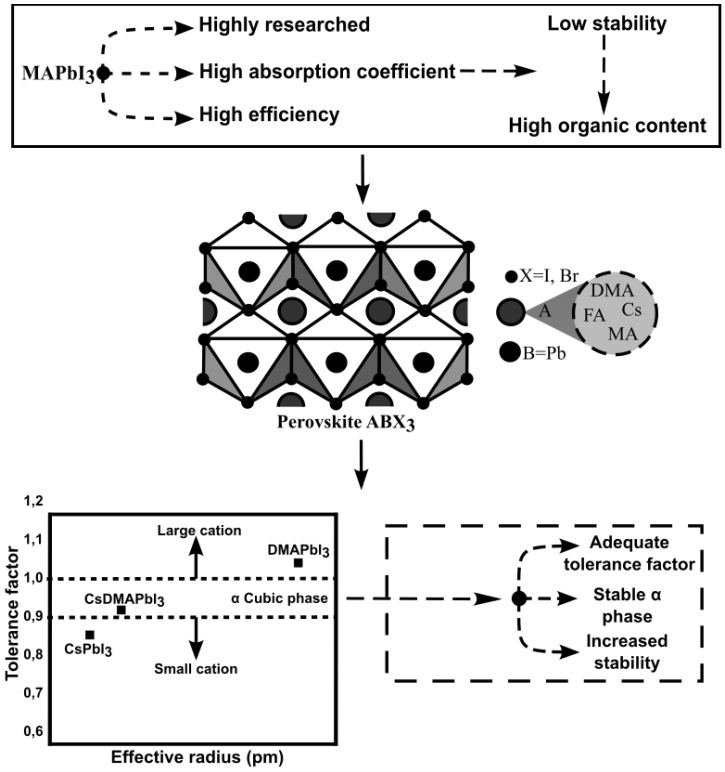

Figure 1. Schematic representation of stability increment by tuning the tolerance factor
Source: own elaboration.

$$t = \frac{R_A + R_x}{\sqrt{2(R_b + R_x)}} \quad (1)$$

In this work, a composition with a significant decrease in the organic component of the perovskite structure ($(Cs_{1-x}DMA_x)Pb(Br_{1-x}I_x)_3$) was studied. A pure phase of this material with morphology suitable for device fabrication was achieved. Additionally, we demonstrated with x-ray diffraction (XRD) analysis that the stability of this composition is considerably higher than that of the $MAPbI_3$ sample. Furthermore, this perovskite was integrated in an optoelectronic device obtaining a PCE of 7.93%. This paper is an extension of the work originally presented at Expo-engineering 2022 [10], which expanded the state of the art, methodology and analysis of results, especially morphological and structural characterization.

1 Materials and methods

1.1 2.1. Materials

N,N-dimethylformamide (DMF) from Sigma Aldrich, hydroiodic acid from Sigma Aldrich, PbI_2 >99.99% from, CsI >99.99%, and $PbBr_2$>99,998% from Alfa Aesar, dimethyl sulfoxide (DMSO) from Sigma Aldrich, $SnCl_2$-$2H_2O$ from Sigma Aldrich, ITO glass, Silver 99%, Spiro-OMeTAD from 1-Material, Lithium salt from Sigma Aldrich, Co (III) TFSI Salt from great cell solar.

1.2 Synthesis of $DMAPbI_3$

This phase is synthesized by the decomposition of DMF in the presence of an acid rich medium (HI), subsequently mixed with the lead precursor (PbI_2). The reaction mechanism is shown in eq. (2), where DMF upon decomposition and mixing with the acid iodide produces DMAI [11]. Finally, DMAI when mixed with lead, forms the $DMAPbI_3$ phase. The mixture contained 1:1 HI to DMF ratio, then PbI_2 with a concentration of 1M was added, the solvent was slowly evaporated in a rotary evaporator for 6 h at 110°C, and faint yellow powders were collected. The summarized preparation process of this phase is shown in Fig. 2.

$$HCON(CH_3)_2 + HI + H_2 \rightarrow (CH_3)_2NH_2I(DMAI) + HCOOH \quad (1)$$

1.3 Synthesis of the perovskite precursor

The precursor of this perovskite was synthesized by mixing the $DMAPbI_3$ phase obtained in the previous step with $PbBr_2$ and CsI in DMF:DMSO 1:1.4. For this purpose, different molar ratios between the components were used to arrive at the purest possible phase. The ratios used were 1:1:2, 1.36:0.74:2, and 0.3:0.7:0.7 respectively, producing the phases $Cs_{0.3}DMA_{0.3}Pb_{0.66}Br_{0.66}I_{1.66}$, $Cs_{0.45}DMA_{0.66}$ $Pb_{0.7}Br_{0.49}$ I_2, and $(Cs_{1-x}DMA_x)Pb(Br_{1-x}I_x)_3$ with x=0.3.

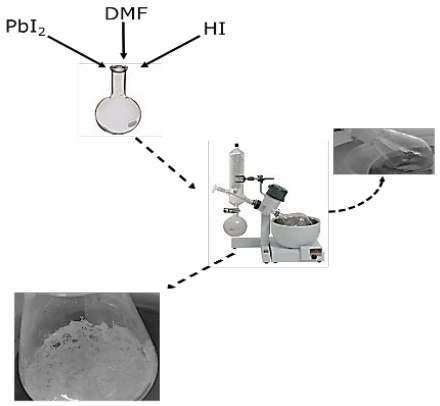

Figure 2. $DMAPbI_3$ Synthesis Process.
Source: own elaboration.

1.4 Solar cell fabrication

The solar cell was fabricated by spin coating, in which the ITO was coated layer by layer under different conditions. Initially, $SnCl_2$-$2H_2O$ dissolved in isopropanol was deposited at a rate of 3000 rpm using the static method. Then, it was annealed at 180 °C for 1 h to obtain SnO_2 used as the electron transport layer (ETL). Then, another SnO_2 layer was deposited by chemical bath synthesis (CBD). Next, perovskite was deposited under different spin-coating conditions as shown in Table 1, followed by two stages of annealing at 70 and 170 °C, this deposition process is schematized in Fig. 3. Subsequently, Co and Li-doped Spiro-OMeOTAD was deposited to form the hole transport layer (HTL) of the solar cell by dynamic spin-coating at 4000 rpm. Finally, a 100 nm thick gold layer was thermally evaporated as an electrode.

Table 1.
Sample deposition parameters.

Concentration (M)	Speed 1 (RPM)	Speed 2 (RPM)	Layer thickness (nm)
1	1000	1000	175
1,3	1000	1000	310
1,3	1000	1500	290
1,3	1000	2500	210

Source: own elaboration.

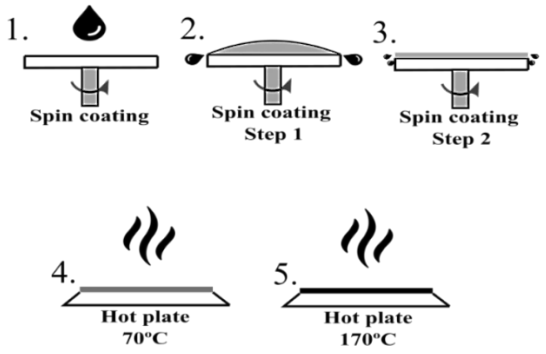

Figure 3. Deposition process of perovskite films.
Source: own elaboration.

1.5 Material Characterization

Xray diffraction (XRD) patterns were acquired on a Rigaku MiniFlex 600. For this, a scan between 2θ= 5° and 65° at a step of 0.01° and speed of 2°/min was used. Cu radiation (λ = 1.5405 Å), with a voltage of 40 kV and a current of 15 mA was employed. The topography of the samples was obtained in an atomic force microscope (AFM) Asyslum Research from OXFORD Instruments with a scan rate of 0.2 Hz, for image processing the WSxM 5.0 software was used [12]. For the optical characterization, absorption and emission spectra were studied by UV-Vis spectroscopy on an Agilent Cary 100 and by photoluminescence (PL) on a Varian fluorescence spectrophotometer, respectively. A profilometer DektakXT Bruker was used to determine the thickness of the deposited layers. Finally, a Keithley 4200SCS and the Oriel sol 3A solar simulator were used to measure the optoelectronic parameters and calibrated under standard AM1.5 conditions using an Oriel 91150-V reference cell.

2 Results and analysis

The relationships between the perovskite cations contribute to different properties of the final structure, where the lower the Cs content the higher the light absorption but lower stability of the α-cubic phase, while for lower DMA content an opposite behavior is observed. Therefore, it is necessary to find the harmony between the cations to obtain a pure phase, with good optoelectronic properties and acceptable stability. For this, different molar ratios such as 1:1:2, 1.36:0.74:2, and 0.3:0.7:0.7 were evaluated for a ratio between the composites $DMAPbI_3$:$PbBr_2$:CsI, producing the phases $Cs_{0.3}DMA_{0.3}Pb_{0.66}Br_{0.66}I_{1.66}$, $Cs_{0.45}DMA_{0.66}Pb_{0.7}Br_{0.49}I_2$, and $(Cs_{1-x}DMA_x)Pb(Br_{1-x}I_x)_3$. It was found that the phases obtained using the composition $Cs_{0.3}DMA_{0.3}Pb_{0.66}Br_{0.66}I_{1.66}$ and $Cs_{0.45}DMA_{0.66}Pb_{0.7}Br_{0.49}I_2$ exhibited high phase mixing with less purity of the final structure, however, the $(Cs_{1-x}DMA_x)Pb(Br_{1-x}I_x)_3$ phase is much purer with the appearance of characteristic peaks in XRD at 14.35° and 29.3° with high intensity, indicating a preferential orientation toward the desired α-phase (Fig. 4) [13]. Additionally, this phase exhibits a reduced background throughout the spectrum, indicating a lower concentration of amorphous phases.

Moreover, in photoluminescence (PL) spectra, the composition producing phase mixture is found to have different emission peaks, indicating active phases with different band gaps. The band gap lower than 1.8 eV belongs to iodine-rich phases with low emissions, appearing around 10° in XRD, and the band gap higher than 2.2 eV to bromine-rich phases (Fig. 5), appearing in XRD between both characteristic peaks (between 14.35° and 29.3°)

Due to the purity of the $(Cs_{1-x}DMA_x)Pb(Br_{1-x}I_x)_3$ phase, the upcoming experiments used this composition. Therefore, the spin coating deposition of the precursor was optimized to obtain films with different thicknesses (as shown in Table 1).

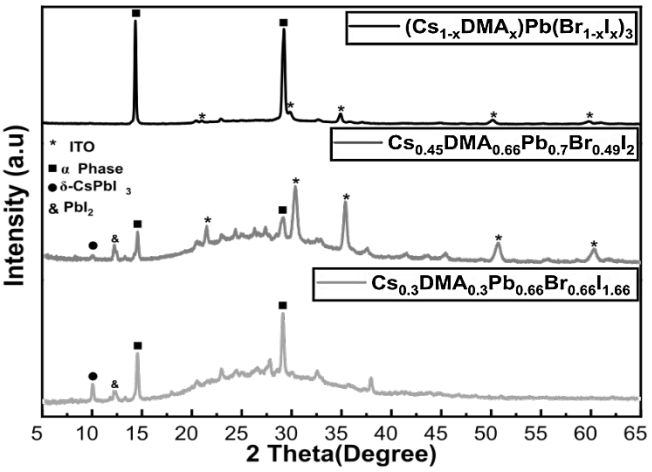

Figure 4. XRD spectra of perovskites with different ion molar ratios. Source: own elaboration.

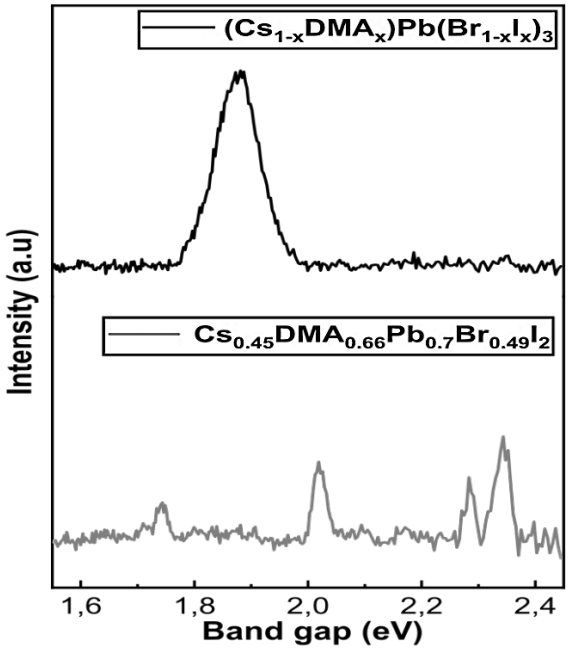

Figure 5. PL photoluminescence spectra at different molar ratios. Source: own elaboration.

This is crucial because thicker films allow high light absorption which could improve the final device efficiency. To confirm this, optical characterization of these layers is performed, observing in the PL spectra an increase in the intensity of the emission peak at higher values of the layer thickness (Fig. 6a), as well as higher absorption in the UV-Vis spectrum (Fig. 6b). This means higher generation of charge carriers in perovskite films of higher thicknesses, producing a better optical behavior [14]. This is promising because perovskites with cations other than MA^+ exhibit a lower absorption coefficient [15]. Therefore, enhancing charge carrier generation by increasing thickness inhibits the detrimental effect of replacing MA^+ on radiation absorption.

To compare this perovskite with the most studied reference ($MAPbI_3$), both perovskites were deposited and evaluated under the same conditions. Initially the AFM topography of both perovskites films was studied, in the case of the perovskite with reduced organic content the typical flake morphology of perovskites with high inorganic content was obtained (Fig. 6c) [13]. However, $MAPbI_3$ perovskite presents spherical grains characteristic of $MAPbI_3$ (Fig. 6d). For this type of materials, it is desirable to have grains as large as possible, providing higher electrical conductivity. In the case of flakes, the average size is about 450 nm. In contrast, the spherical grains size is around 150 nm, indicating a promising morphology of the perovskite under study.

To maintain the α-phase shown in XRD, it is desired to combine organic and inorganic cations in order to obtain a tolerance factor that yields pure cubic phase with geometric stability. For this purpose, the $CsPbI_3$ perovskite was explored together with bromine and the organic perovskite $DMAPbI_3$. The $CsPbI_3$ structure has a very low tolerance factor leading to rapid decomposition under ambient conditions; on the other hand, $DMAPbI_3$ is a structure with a tolerance factor higher than one and undesirable optoelectronic properties.

However, the combination of $CsPbI_3$ and $DMAPbI_3$ perovskites yield a structure with a tolerance factor in the ideal zone between 0.9 and 1, where the α-cubic phase necessary to maintain perovskite integrity for a longer time is produced. Combining these two cations increases the geometrical stability due to the size of the cations, which balances the structure and possibly the associated internal stresses. Li, Zhen et al. demonstrated that adding DMA to inorganic components such as cesium reduces the annealing temperature of perovskites, achieving the transition from the yellow δ phase to the black α phase at lower temperature [9]. This has also been evidenced in other reports suggesting that both the formation energy and the tolerance factor are favored by cation tuning leading to structural stability of the phase [11,16-18].

Now, analyzing the XRD of each of these conditions, it is found that there is a good reproducibility of the obtained phases (Fig. 7). However, the main peak at 14.35° indicates that the deposition conditions of higher spin coating velocity generate larger crystallite sizes, while lower velocities lead to thicker layers and smaller crystallite size (Table 2). This can be explained by changes in the evaporation rate during the process, leading to different nucleation points and crystallite growth rate. It is recommended in future works to continue the crystallization analysis to favor the increase in crystallite size at higher layer thickness, promoting the decrease in charge transfer resistance at the best thickness condition. This can be done with various additives that facilitate the increase in crystallite and grain size [19,20,21].

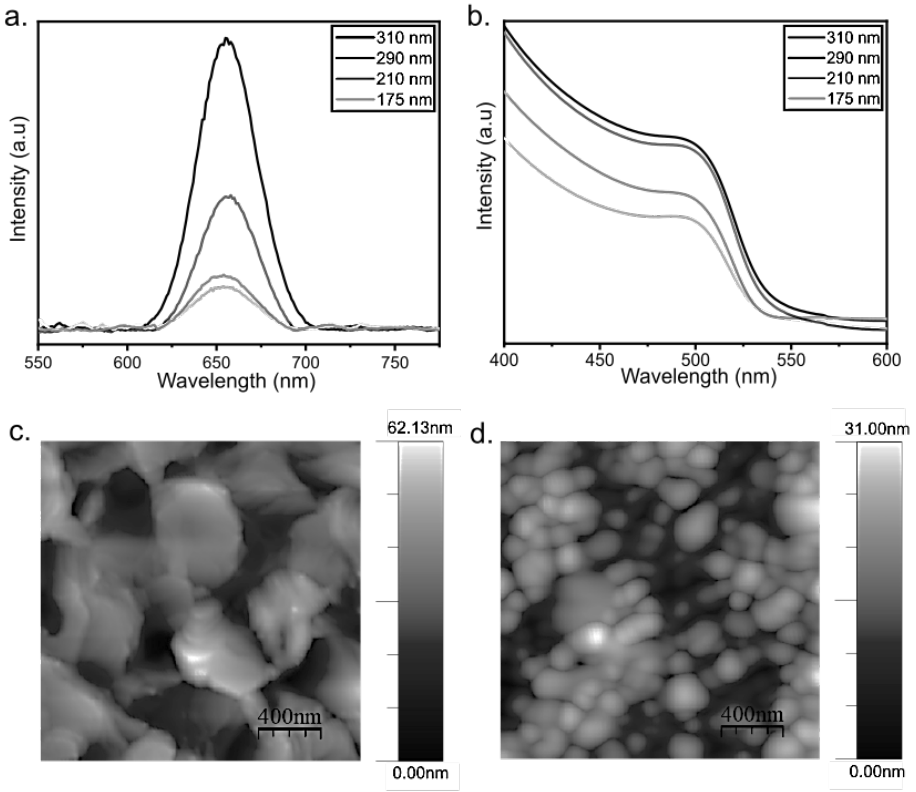

Figure 6. a. PL spectra of perovskite films at different thicknesses, b. UV-Vis spectra of perovskite films at different thicknesses, c. AFM image of perovskite $(Cs_{1-x}DMA_x)Pb(Br_{1-x}I_x)_3$, AFM image of perovskite $MAPbI_3$ (Scale 400 nm).
Source: own elaboration.

Table 2.
Crystallite size at different deposition conditions

Thickness (nm)	FWHM	Crystallite size (nm)
310	0,226	35,339
290	0,228	35,125
210	0,214	37,401
175	0,193	41,509

Source: own elaboration.

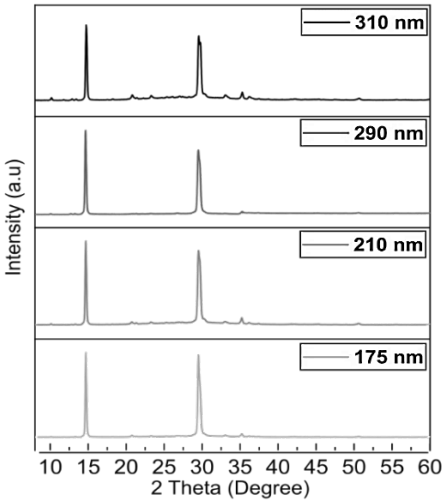

Figure 7. XRD spectra of perovskite at different thicknesses Source: own elaboration.

To correlate the variables studied here with the optoelectronic properties of the device, the solar cells described in the methodology section are made and compared with $MAPbI_3$ as the reference perovskite (Fig. 8). We observed that on average the photovoltaic parameters closer to the reference correspond to the active layers with greater thickness, due to a better absorption of light. This is critical because this perovskite has a lower absorption coefficient than $MAPbI_3$. Therefore, the thickness must be increased to provide a charge production comparable to that of $MAPbI_3$.

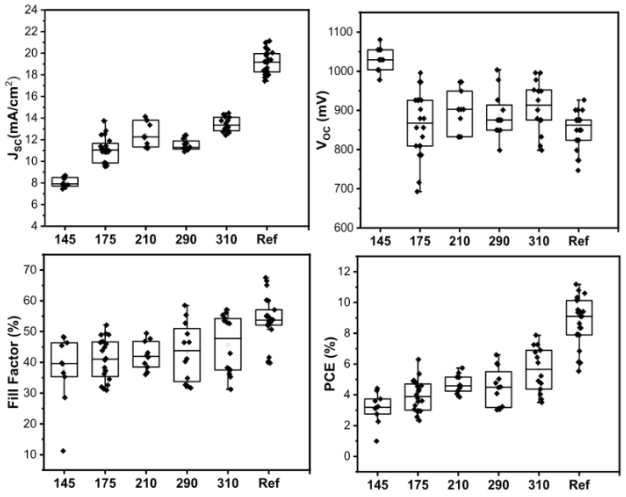

Figure 8. Box charts of photovoltaic parameters of perovskite solar cells with different active layer thicknesses (nm).
Source: own elaboration.

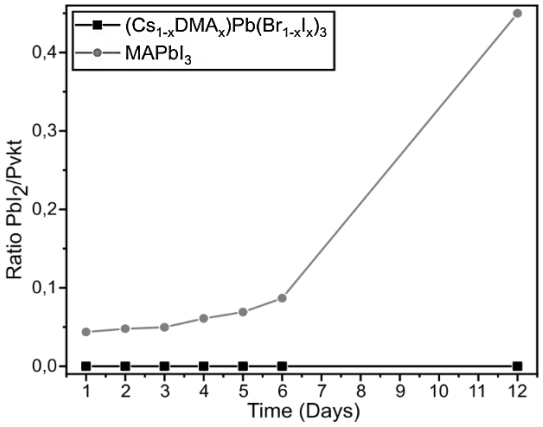

Figure 9. Comparative plot of the PbI_2/Pvkt ratio in the perovskite $(Cs_{1-x}DMA_x)Pb(Br_{1-x}I_x)_3$ and the reference. Study carried out at 30-40% relative humidity Source: own elaboration.

Finally, the stability of the $(Cs_{1-x}DMA_x)Pb(Br_{1-x}I_x)_3$ perovskite was studied by comparing it with that of $MAPbI_3$, where we observed that the time evolution of the PbI_2 peak in the XRD spectra is significantly higher in $MAPbI_3$ than in $(Cs_{1-x}DMA_x)Pb(Br_{1-x}I_x)_3$ (Fig. 9). This indicates that the degradation rate at the conditions under study of $MAPbI_3$ perovskite is higher than in $(Cs_{1-x}DMA_x)Pb(Br_{1-x}I_x)_3$ perovskite. This figure shows that after 12 days, the $MAPbI_3$ perovskite is considerably damaged by the returning to its main precursor, PbI_2 however, the $(Cs_{1-x}DMA_x)Pb(Br_{1-x}I_x)_3$ has not started to degrade yet.

1 Conclusions

Inorganic perovskites that minimize the organic component in their composition exhibit adequate properties and morphologies that address the fundamental stability issues of this class of semiconductors. In this study, we conclude that the most critical parameters to control are the layer thickness, morphology, and phase. This is due to the significant differences in optical properties, such as bandgap, and absorption coefficient, compared to conventional perovskites. Thus, finding appropriate parameters for depositing a high-purity layer that can be integrated into optoelectronic devices is crucial. Our results indicate that optimizing the process by adjusting molar ratios, perovskite concentration, and spin-coating parameters is necessary to control these variables.

Specifically, we developed an experimental procedure for depositing 300 nm $(Cs_{1-x}DMA_x)Pb(Br_{1-x}I_x)_3$ perovskite layers that resulted in a pure phase material with the desired thickness and optical absorption properties. We used these layers to fabricate solar cells that achieved an average power conversion efficiency (PCE) of approximately 7.9%, which is equivalent to 80% of the PCE of the reference device.

Acknowledgements

The authors thank Minciencias by the financial support of this work under the contract 177-2021.

References

[1] RNEA, Renewable Power Generation Costs in 2020. 2020.

[2] Shi, B., Duan, L., Zhao, Y., Luo, J., and Zhang, X., Semitransparent perovskite solar cells: from materials and devices to applications, Adv. Mater., 32(3), pp. 1-12, 2020. DOI: https://doi.org/10.1002/adma.201806474.

[3] Wang J., et al., Highly efficient all-inorganic perovskite solar cells with suppressed non-radiative recombination by a Lewis base, Nat. Commun., 11(1), pp. 1-9, 2020. DOI: https://doi.org/10.1038/s41467-019-13909-5.

[4] Li Z., et al., Ammonia for post-healing of formamidinium-based Perovskite films, Nat. Commun., 13(1), pp. 1-10, 2022. DOI: https://doi.org/10.1038/s41467-022-32047-z.

[5] Zhu X. et al., Superior stability for perovskite solar cells with 20% efficiency using vacuum co-evaporation, Nanoscale, 9(34), pp. 12316-12323, 2017. DOI: https://doi.org/10.1039/c7nr04501h.

[6] Tong G. et al., Phase transition induced recrystallization and low surface potential barrier leading to 10.91%-efficient CsPbBr3 perovskite solar cells, Nano Energy, 65(June), art. 104015, 2019. DOI: https://doi.org/10.1016/j.nanoen.2019.104015.

[7] Wang Y. et al., The role of Dimethylammonium Iodide in CsPbI3 Perovskite fabrication: additive or dopant?, Angew. Chemie - Int. Ed., 58(46), pp. 16691-16696, 2019. DOI: https://doi.org/10.1002/anie.201910800.

[8] Liu C. et al., Promising applications of wide bandgap inorganic perovskites in underwater photovoltaic cells, Sol. Energy, 233(June) 2021, pp. 489-493, 2022. DOI: https://doi.org/10.1016/j.solener.2022.01.033.

[9] Li, Z., Yang, M., Park, J.S., Wei, S.H., Berry, J.J. and Zhu, K., Stabilizing Perovskite structures by tuning tolerance factor: formation of Formamidinium and Cesium lead Iodide solid-state alloys, Chem. Mater., 28(1), pp. 284-292, 2016. DOI: https://doi.org/10.1021/acs.chemmater.5b04107.

[10] Engineering, V., Engineering for transformation: hybrid Perovskite (Cs1-xDMA x) Pb(Br1-xI x)3 solar cells with improved stability. Fondo Editorial EIA, Envigado, Colombia, 2022.

[11] Ke, W., Spanopoulos, I., Stoumpos, C.C. and Kanatzidis, M.G., Myths and reality of HPbI3 in halide perovskite solar cells, Nat. Commun., 9(1), 2018. DOI: https://doi.org/10.1038/s41467-018-07204-y.

[12] Horcas, I., Fernández, R., Gómez-Rodríguez, J.M., Colchero, J., Gómez-Herrero, J. and Baro, A.M., WSXM: a software for scanning probe microscopy and a tool for nanotechnology, Rev. Sci. Instrum., 78(1), art. 2410, 2007. DOI: https://doi.org/10.1063/1.2432410.

[13] Wang, H., Liu, H., Dong, Z., Li, W., Zhu, L. and Chen, H., Composition manipulation boosts the efficiency of carbon-based CsPbI3 perovskite solar cells to beyond 14%," Nano Energy, 84(January), art. 105881, 2021. DOI: https://doi.org/10.1016/j.nanoen.2021.105881.

[14] Mishra A. et al., Interplay of kinetic and thermodynamic reaction control explains incorporation of Dimethylammonium Iodide into CsPbI3, ACS Energy Lett., 7(8), pp. 2745-2752, 2022. DOI: https://doi.org/10.1021/acsenergylett.2c00877.

[15] Bouich, A., Marí-Guaita, J., Baig, F., Hameed-Khattak, Y., Soucase, B.M. and Palacios, P., Investigation of the surface coating, humidity degradation, and recovery of Perovskite film phase for solar-cell applications, Nanomaterials, 12(17), art. 173027, 2022. DOI: https://doi.org/10.3390/nano12173027.

[16] Marshall A.R. et al., Dimethylammonium: an a-site cation for modifying CsPbI3, Sol. RRL, 5(1), art. 000599, 2021. DOI: https://doi.org/10.1002/solr.202000599.

[17] Fu Y. et al., Incorporating large a cations into lead Iodide Perovskite cages: relaxed Goldschmidt tolerance factor and impact on exciton-phonon interaction, ACS Cent. Sci., 5(8), pp. 1377-1386, 2019. DOI: https://doi.org/10.1021/acscentsci.9b00367.

[18] Li Z. et al., Scalable fabrication of perovskite solar cells, Nat. Rev. Mater., 3, pp. 1-20, 2018. DOI: https://doi.org/10.1038/natrevmats.2018.17.

[19] Chen, S., Dai, X., Xu, S., Jiao, H., Zhao, L. and Huang, J., Stabilizing perovskite-substrate interfaces for high-performance perovskite modules, Science 373(6557), pp. 902-907, 2021. DOI: https://doi.org/10.1126/science.abi6323.

[20] Deng, Y., van Brackle, C.H., Dai, X., Zhao, J., Chen, B. and Huang, J., Tailoring solvent coordination for high-speed, room-temperature blading of perovskite photovoltaic films, Sci. Adv., 5(12), pp. 1-9, 2019. DOI: https://doi.org/10.1126/sciadv.aax7537.

[21] Deng, Y., Xu, S., Chen, S., Xiao, X., Zhao, J. and Huang, J., Defect compensation in formamidinium-caesium Perovskites for highly efficient solar mini-modules with improved photostability, Nat. Energy, 6(6), pp. 633-641, 2021. DOI: https://doi.org/10.1038/s41560-021-00831-8.

J.J. Patiño-López, received the BSc. Eng. in Materials Engineer and member of the Center for Research, Innovation and Development of Materials - CIDEMAT of the University of received the Antioquia, Colombia. He has participated in projects for developing perovskite-based solar cells for their application in the generation of green hydrogen.
ORCID: 0000-0002-5518-2265

J.F. Montoya-Arango, BSc. Eng. and MSc. in Chemical Engineering from the University of Antioquia in 2006 and 2009, respectively. He obtained a PhD in Chemistry in 2013, from the Autonomous University of Barcelona, Spain. He is currently a professor in the Department of Materials Engineering and member of the Center of Research, Innovation and Development of Materials – CIDEMAT at the Universidad de Antioquia, Colombia. His research interests include photocatalysis and nanostructured solar cells. He is currently working on synthesis and characterization of nanomaterials and thin films for scalable perovskite solar cells and green hydrogen production applications.
ORCID: 0000-0002-6236-8922

E.A. Ramírez-Pérez, received the BSc. Eng. in Chemical Engineering in 2012, from the Industrial University of Santander, Colombia. He completed a MSc. in Nanomaterials in 2017, from the University of Zaragoza and a PhD in Materials Engineering in 2019, from the Universidad Nacional de Colombia. He is currently a researcher at the Center for Research, Innovation and Development of Materials - CIDEMAT at the Universidad de Antioquia, Colombia. He is currently researching in the manufacture of perovskite cells by scalable printing methods, the encapsulation of solar devices and their integration with devices for the generation of H2.
ORCID: 0000-0002-4770-5986

F. Jaramillo-Isaza, received the BSc. Eng. in Chemical Engineering in 2002, from the University of Antioquia, Colombia, and PhD. in Chemistry in 2005, from the University of Manchester, England. He is currently a full professor in the Department of Materials Engineering and member of the Center of Research, Innovation and Development of Materials – CIDEMAT at Universidad de Antioquia, Colombia. His research interests include materials for energy, nanostructured solar cells and processing techniques. He is the scientific director of the Energy Sustainability for Colombia Program – Séneca.
ORCID: 0000-0003-1722-5487

D.E. Ramirez-Zora, received the BSc. Eng. and PhD. in Materials Engineering in 2014 and 2018 respectively, from the University of Antioquia, Colombia. He is currently a professor in the Department of Materials Engineering and member of the Center of Research, Innovation and Development of Materials – CIDEMAT at the Universidad de Antioquia. His research interests include nanotechnology and nanostructured solar cells. He is currently working on synthesis and characterization of nanoparticles, nanocomposites and novel semiconductors for scalable perovskite solar cells and green hydrogen production applications.
ORCID: 0000-0003-2630-7628